Cold-induced Spreading of Water Drops on Hydrophobic Surfaces

Faryar Tavakoli and H. Pirouz Kavehpour[1]

[1]Department of Mechanical and Aerospace Engineering, University of California – Los Angeles (UCLA), Los Angeles, California 90024, USA

Presented at the 17th International Coating Science and Technology Symposium

September 7-10, 2014

San Diego, CA, USA

Introduction:

Hydrophobic surfaces are universally used for their unique self-cleaning properties, as water droplets roll along these surfaces rather than spread. There have been many studies in the last decade on capability of hydrophobic surfaces to induce a significant delay on freezing or ice adhesion reduction at extreme cold conditions[1-7]. However, in practice, the efficiency of the hydrophobic surfaces under conditions of extreme humidity, airflow[5], particle diameter of the hydrophobic surface[8], icing/deicing cycles[9], and frost formation[6] is critically questioned. Despite the obvious influence of contact angle and base diameter of the drop on the ice adhesion[10-13] and freezing time[14,15] of the supercooled drops, a systematic investigation on wetting dynamics of water drops on hydrophobic surfaces during the cooling stage, prior to freezing initiation, has not been conducted. Few studies about the thermal stability of hydrophbic surfaces have been published[16-18].

The present study aims to investigate the drop movement caused by cold hydrophobic substrates and unveil the underlying mechanism. The effects of the substrate temperature, humidity, types of hydrophobic surfaces, drop volume and the surface roughness on the movement is explored. The solid-liquid-gas line (trijunction) during the spreading is monitored closely using a high–speed camera to track the movement closely.

Experimental Set up and Materials:

The hydrophobic surfaces, on which water drops are deposited, were cooled by a Peltier element. The Peltier element is situated in a Drop Shape Analyzer (DSA100, krüss) machine to accurately observe the dynamics. Cooling rate is kept constant by circulation of coolant water with predetermined temperature around the hot side of the Peltier element. Four different kinds of hydrophobic surfaces of WX2100™, Fluorothane™, Silicon pillars and Teflon, with equilibrium angles of 144°±1.8, 142°±1.5, 149°±1.3 and 108°±2.1 were used, respectively. The area fraction of the solid surface in contact with water (ϕ_s) and roughness factor (r) for the silicon pillars are 0.26 and 1.15, respectively. Both WX2100™ (aerosol coating) and Fluorothane™ (solution coating) are applied to the surface of cover glasses. It is worth mentioning that the thickness of applied WX2100™ spray and applied Fluorothane™ solution on the cover glasses do not change the wetting characteristics significantly.

Results and Discussion:

In order to evaluate the role of the substrate temperature, water drops with constant volume of 9μL are cooled from 25°C to assigned temperatures of 15°C, 10°C, 0°C, -10°C and -20°C on a cover glass coated with WX2100™ at relative humidity of 18%. During the cooling process, the drops start spreading gradually and smoothly over the solid substrate. No variation of contact angle and base diameter is observed for temperatures ranging from RT to 15°C; however, cooling below 15°C, the final diameter and apparent contact angle of the drop is dependent on the

substrate temperature (FIG. 1). Elapsed time to spreading initiation is independent from the assigned temperature; however, colder substrates amplified spreading rates with larger post-spreading footprint (FIG. 1). Depinning followed by spreading occurred at both right and left contact angles, rather than rolling in one direction.

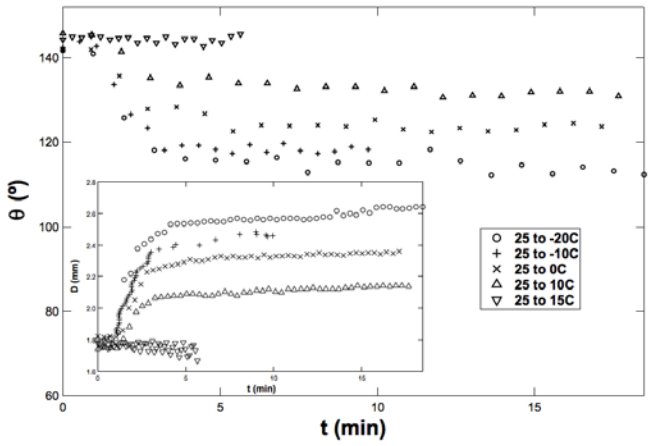

FIG. 1. Apparent contact angle of 9μl water drops versus time on WX2100 substrate cooled by a Peltier element to temperatures of 15°C, 10°C, 0°C, -10°C and -20°C at 18 RH%. Inset shows associated drop diameter versus time.

To elucidate the effect of humidity on cold-induced spreading, for a constant change in substrate temperature (25°C to -10°C), humidity was adjusted by using a nitrogen flux into the closed chamber of DSA100 apparatus. First, relative humidity is stabilized in the chamber and then cooling of Peltier element is started. Drop-spreading dynamics showed a significant dependency on humidity. Higher humidity facilitates the spreading onset and increases the final diameter of the water drop. Higher humidity results in larger driving force for capillary condensation at the trijunction that accelerates condensation initiation and growth. In the growth phase of the condensates in the form of a thin film, vapor phase condensation and evaporation from the water drop both contribute to the dynamics.

A simple and inexpensive procedure to fabricate hydrophobic surfaces from Teflon, introduced by Nilsson et al[19]., is followed to examine the effect of roughness. In this method, Teflon surfaces are sanded using different grit designations and subsequent cleaning of solid Teflon. Grit sizes correspond to the size of the particles and distance of the abrading particles embedded on the sandpaper. The higher the grit number, the smoother the sandpaper. Water drops with constant volume of 9μL are deposited on a Peltier element situated in the DSA machine. The water drops are cooled to temperatures below zero degrees. Figure 2 shows the spread factor, ratio of the post-spreading drop diameter (D_f) to the initial diameter (D_0), versus grit size. Six data points are collected for each designated sanded Teflon. Ratio of post-spreading diameter versus initial diameter increases with the surface roughness, except for 120-grit size. The change of behavior from 220 to 120-grit size is attributed to extra coarse structure that acts as a resisting force to inception and continuation of the spreading.

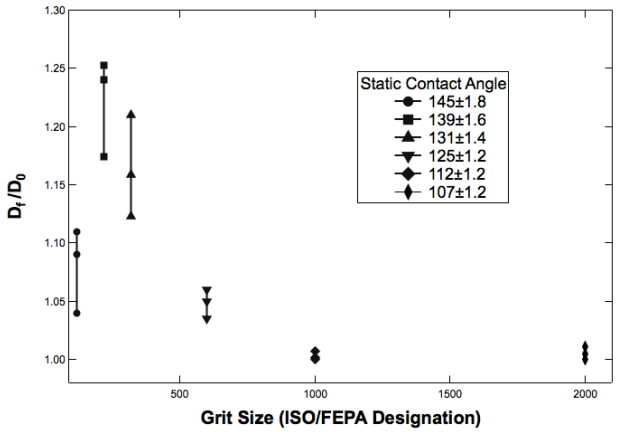

FIG. 2. Dimensionless diameter, post-spreading diameter to initial diameter, of the water drops cooled to -10°C versus grit size used for sanding the Teflon surface. Lower grit sizes of sandpaper correspond to finer roughness.

Different volumes of the water drops are deposited on the WX2100 coated surface and cooled to -10°C using a Peltier element. The diameter of the water drops ranges from 0.47 to 11.22mm with the same initial contact angle of 144°±1.8. Figure 3 depicts the diameter of water drops on cooling WX2100 coated surface versus time for multiple drop volumes. At constant humidity and definite temperature change, the spreading kinetics and initiation at relatively large length scale is only a function of contact angle (Figure 3). Elapsed time to depinning of 556μL, 180.8μL, 66μL, 39μL, 9μL, 4.1μL, and 0.3μL drops are 36.3±2.1, 42.5±2.8, 32.05±3.4, 37.5±3.3, 57.6±3.3, 67.6±4.2 and 126.7±4.5 s, respectively. For water drops smaller than the capillary length, time to drop depinnig increases, because surface forces become more dominant in this length scale. Capillary length is defined as $L_{cap} = \sqrt{\sigma/\rho g}$, where σ is surface tension, ρ is the liquid density, and *g* is the gravitational acceleration. For deionized water, capillary length is 2.7mm. For smaller drops in micrometer range, the Van der Waals (vdW) forces become controlling. Both water drops with base diameters of 0.47mm and 1.14mm depinned at longer timescales with respect to drops larger than capillary length. Independency of elapsed time to depinnig of the water drops to various volume sizes with the same contact angle, except for water drops that smaller than capillary length at which capillary and vdW forces are important, signifies the effect of surface forces such as capillary/premature condensation around the confined region rather than bulk forces that depends on the drop volume.

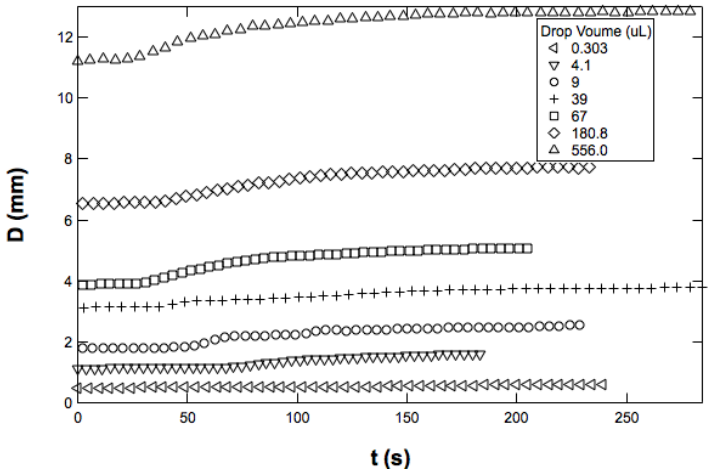

FIG. 3. Apparent diameter of the water drops on cooling WX2100 coated surfaces versus time for different drop volumes.

Conclusions:

In sum, we studied the cold-induced dynamics of sessile water drops on cooling hydrophobic substrates. The water drops on cooling hydrophobic surfaces depin and start to spread (up to 33% of the initial diameter) on cooling hydrophobic surfaces. This cold-induced spreading is found to be strongly dependent on the substrate temperature, relative humidity of surrounding air, and initial contact angle of the drop. From the physical parameters studied and visually monitoring the trijunction region during spreading, the spreading is due to premature condensation and formation of a liquid rim at the trijunction followed by the film propagation radially away from the drop. During the growth phase of the thin film, the drop depins and starts spreading gradually on the film. Lower temperatures of the hydrophobic substrate resulted in more spreading of the drops; however, different designated temperatures have not affected the time to spreading initiation. Higher humidity of surrounding air facilitated the onset of spreading with larger final footprint of the drops. Introducing roughness to the hydrophobic surfaces lead to higher post-spreading diameter; whereas, extremely coarse surfaces impede cold-induced spreading. Drops with smaller base diameter than Capillary length of water spread less due to pinning effect stemmed from strong capillary and even vdW forces.

The results corroborate the influence of many parameters such as the relative humidity, surface roughness, initial contact angle and the drop volume on the temperature-induced spreading of water drops on cooling hydrophobic surfaces. This will be of great importance in the design, assessment and development of superhydrophobic materials for freezing-delay and anti-icing applications such as aircrafts, wind turbines, and high-voltage power lines.

References:

(1) Li, K. Y.; Xu, S.; Shi, W. X.; He, M.; Li, H. L.; Li, S. Z.; Zhou, X.; Wang, J. J.; Song, Y. L. Investigating the effects of solid surfaces on ice nucleation. *Langmuir* **2012**, 28, 10749-10754.
(2) Tourkine, P.; Le Merrer, M.; Quere, D. Delayed freezing on water repellent materials. *Langmuir* **2009**, 25, 7214-7216.
(3) He, M.; Wang, J.; Li, H.; Jin, X.; Wang, J.; Liu, B.; Song, Y. Super-hydrophobic film retards frost formation. *Soft Matter* **2010**, 6, 2396-2399.
(4) Jung, S.; Dorrestijn, M.; Raps, D.; Das, A.; Megaridis, C. M.; Poulikakos, D. Are superhydrophobic surfaces best for icephobicity? *Langmuir* **2011**, 27, 3059-3066.
(5) Jung, S.; Tiwari, M. K.; Doan, N. V.; Poulikakos, D. Mechanism of supercooled droplet freezing on surfaces. *Nat. Commun.* **2012**, 3.
(6) Varanasi, K. K.; Deng, T.; Smith, J. D.; Hsu, M.; Bhate, N. Frost formation and ice adhesion on superhydrophobic surfaces. *Applied Physics Letters* **2010**, 97.

(7) Hao, W.; Liming, T.; Xiaomin, W.; Wantian, D.; Yipeng, Q. Fabrication and anti-frosting performance of super hydrophobic coating based on modified nano-sized calcium carbonate and ordinary polyacrylate. *Appl. Surf. Sci.* **2007**, 253, 8818-8824.
(8) Cao, L. L.; Jones, A. K.; Sikka, V. K.; Wu, J. Z.; Gao, D. Anti-icing superhydrophobic coatings. *Langmuir* **2009**, 25, 12444-12448.
(9) Kulinich, S. A.; Farhadi, S.; Nose, K.; Du, X. W. Superhydrophobic surfaces: Are they really ice-repellent? *Langmuir* **2011**, 27, 25-29.
(10) Mobarakeh, L. F.; Jafari, R.; Farzaneh, M. The ice repellency of plasma polymerized hexamethyldisiloxane coating. *Appl. Surf. Sci.* **2013**, 284, 459-463.
(11) Liang, G.; Guifu, D.; Hong, W.; Jinyuan, Y.; Ping, C.; Yan, W. Anti-icing property of superhydrophobic octadecyltrichlorosilane film and its ice adhesion strength. *J. Nanomater.* **2013**, 278936 (5 pp.)-278936 (5 pp.).
(12) Dotan, A.; Dodiuk, H.; Laforte, C.; Kenig, S. The relationship between water wetting and ice adhesion. *J. Adhes. Sci. Technol.* **2009**, 23, 1907-1915.
(13) Meuler, A. J.; Smith, J. D.; Varanasi, K. K.; Mabry, J. M.; McKinley, G. H.; Cohen, R. E. Relationships between water wettability and ice adhesion. *ACS Appl. Mater. Interfaces* **2010**, 2, 3100-3110.
(14) Huang, L. Y.; Liu, Z. L.; Liu, Y. M.; Gou, Y. J.; Wang, L. Effect of contact angle on water droplet freezing process on a cold flat surface. *Exp. Therm. Fluid Sci.* **2012**, 40, 74-80.
(15) Boinovich, L.; Emelyanenko, A. M.; Korolev, V. V.; Pashinin, A. S. Effect of wettability on sessile drop freezing: When superhydrophobicity stimulates an extreme freezing delay. *Langmuir* **2014**, 30, 1659-1668.
(16) Mockenhaupt, B.; Ensikat, H. J.; Spaeth, M.; Barthlott, W. Superhydrophobicity of biological and technical surfaces under moisture condensation: Stability in relation to surface structure. *Langmuir* **2008**, 24, 13591-13597.
(17) Wang, F. C.; Li, C. R.; Lv, Y. Z.; Lv, F. C.; Du, Y. F. Ice accretion on superhydrophobic aluminum surfaces under low-temperature conditions. *Cold Reg. Sci. Tech.* **2010**, 62, 29-33.
(18) Karmouch, R.; Ross, G. G. Experimental study on the evolution of contact angles with temperature near the freezing point. *Journal of Physical Chemistry C* **2010**, 114, 4063-4066.
(19) Nilsson, M. A.; Daniello, R. J.; Rothstein, J. P. A novel and inexpensive technique for creating superhydrophobic surfaces using teflon and sandpaper. *J. Phys. D-Appl. Phys.* **2010**, 43.